Electronic Reconstruction at the Isopolar $LaTiO_3/LaFeO_3$ Interface: An X-Ray Photoemission and Density-Functional Theory Study

J. E. Kleibeuker,[1,2,*] Z. Zhong,[3] H. Nishikawa,[4] J. Gabel,[2] A. Müller,[2] F. Pfaff,[2] M. Sing,[2] K. Held,[3] R. Claessen,[2] G. Koster,[1] and G. Rijnders[1]

[1]*Faculty of Science and Technology and MESA+Institute for Nanotechnology, University of Twente, 7500 AE Enschede, Netherlands*
[2]*Physikalisches Institut, University of Würzburg, 97074 Würzburg, Germany*
[3]*Institute of Solid State Physics, Vienna University of Technology, A-1040 Vienna, Austria*
[4]*Faculty of Biology-Oriented Science and Technology, Kinki University, Kinokawa 649-6493, Japan*

(Received 14 April 2014; published 2 December 2014)

We report the formation of a nonmagnetic band insulator at the isopolar interface between the antiferromagnetic Mott-Hubbard insulator $LaTiO_3$ and the antiferromagnetic charge transfer insulator $LaFeO_3$. By density-functional theory calculations, we find that the formation of this interface state is driven by the combination of O band alignment and crystal field splitting energy of the t_{2g} and e_g bands. As a result of these two driving forces, the Fe $3d$ bands rearrange and electrons are transferred from Ti to Fe. This picture is supported by x-ray photoelectron spectroscopy, which confirms the rearrangement of the Fe $3d$ bands and reveals an unprecedented charge transfer up to 1.2 ± 0.2 e^-/interface unit cell in our $LaTiO_3/LaFeO_3$ heterostructures.

DOI: 10.1103/PhysRevLett.113.237402 PACS numbers: 78.70.Dm, 71.15.Mb, 73.40.-c, 79.60.Jv

Complex oxide heterointerfaces exhibit unique properties which are absent in the corresponding isolated parent compounds [1–3]. For example, metallic interfaces have been achieved between a polar and a nonpolar insulating perovskite oxide (ABO_3), e.g., at $LaAlO_3/SrTiO_3$, $LaTiO_3/SrTiO_3$, and $GdTiO_3/SrTiO_3$ interfaces [3–5]. To clarify this metallic behavior, intrinsic electronic reconstruction is suggested to compensate the interfacial polar discontinuity, resulting in a quasi-two-dimensional electron gas at the heterointerface [6–8]. However, competing mechanisms have often been proposed to act and obscure the sought-after electronic reconstruction. For example, the formation of oxygen vacancies has been shown to play an important role in the titanate-based metallic interfacial systems [9–12]. To achieve full understanding of charge transfer, it is necessary to investigate a perovskite interface where distinct phenomena allow us to unequivocally identify the proposed charge transfer mechanism. A perovskite heterostructure where defects play no role in the physical properties is desired. Subsequently, the achieved knowledge on charge transfer in this model system can be extended to other perovskite interface systems.

In this Letter, we therefore focus on internal charge transfer at the isopolar insulating interface between $LaTiO_3$ and $LaFeO_3$, where $LaTiO_3$ is a Mott-Hubbard insulator (MHI) and $LaFeO_3$ is a charge transfer insulator (CTI) [13]. The advantage of this heterostructure is the absence of polar discontinuity at the interface. In addition, both bulk $LaFeO_3$ and bulk $LaTiO_3$ have a partially filled $3d$ transition metal ion on the B site. This offers the opportunity to exploit the differences in band configuration of $LaTiO_3$ and $LaFeO_3$ near the Fermi level to drive electronic reconstruction.

For $LaFeO_3$, the charge transfer gap (Δ) is determined by the filled oxygen $2p$ band and the unoccupied upper Hubbard $3d$ band of Fe ($\Delta_{CT} = 2.2$ eV) [13,14]. For $LaTiO_3$, the gap originates from the Mott-Hubbard splitting of the Ti d bands ($\Delta_{MH} = 0.2$ eV), while the oxygen $2p$ band is located below the partially filled d band ($\Delta_{CT} = 4.5$ eV) [13,14]. In $LaTiO_3/LaFeO_3$ heterostructures, alignment of the O bands is expected to occur at the interface, as the two materials share their oxygen atoms at the interface [15]. As a result of this band alignment, the empty upper d band of $LaFeO_3$ is expected to be pushed below the energy level of the partially filled lower d band of $LaTiO_3$, which would favor electron transfer from Ti to Fe, i.e., interfacial electronic reconstruction. Let us note that a charge transfer in 1/1 $LaNiO_3/LaTiO_3$ (CTI/MHI) superlattices has recently been studied by Chen *et al.*, using density-functional theory (DFT) + U [15]. The authors found that a charge transfer from Ti to Ni enhances correlation effects and leads to a Mott insulator with an enhanced moment of $S = 1$ on the Ni sites and a charge transfer gap between Ni and (empty) Ti d states.

Based on our DFT calculations, we present clear evidence that, besides the presence of oxygen band alignment, the competition with crystal field and correlation energy of the d electrons is crucial to achieve electronic reconstruction at MHI/CTI interfaces. At $LaTiO_3/LaFeO_3$ interfaces, this competition results in both charge transfer and a rearrangement of the Fe bands which can lead to a new nonmagnetic band insulating state at the interface. Using *in situ* x-ray photoelectron spectroscopy (XPS), we confirm the charge transfer and band rearrangement experimentally. By fitting the XPS

data, we have determined an electron transfer up to 1.2 ± 0.2 per interface unit cell (u.c.) from Ti to Fe.

For the DFT calculations, we employed the local density approximation (LDA) and the projector augmented-wave method as implemented in the Vienna *ab initio* simulation package (VASP) [16,17]. A kinetic energy cutoff of 500 eV was used and the Brillouin zone was sampled with an $8 \times 8 \times 6$ k-point grid in combination with a tetrahedron method. Including an on-site Coulomb interaction, the LDA + U calculated ground states and energy gaps for bulk $LaTiO_3$ and $LaFeO_3$ agree well with experiments for an optimized $U_d^{\mathrm{Ti}} = 3.0$ eV and $U_d^{\mathrm{Fe}} = 4.8$ eV, respectively [see Figs. 1(a) and 1(b)] [18–20]. Bulk $LaTiO_3$ had a MHI-type energy gap between the filled and unfilled Ti t_{2g} states and bulk $LaFeO_3$ had a CTI-type energy gap between the filled O $2p$ states hybridized to Fe e_g states and the unfilled Fe t_{2g} states [21]. Both bulk materials were G-type antiferromagnetic. Subsequently, we modeled (1/1), (2/2), and (2/4) $LaTiO_3/LaFeO_3$ heterostructures using a periodically repeated supercell [22]. The unit cells had a $GdFeO_3$-type distorted orthorhombic structure and the lattice constants were fixed at the optimized $LaTiO_3$ bulk values [21]. The atoms were allowed to relax internally. To integrate these distortions in $LaTiO_3/LaFeO_3$ superlattices, we replaced one Ti atom of the distorted $LaTiO_3$ structure, which has a $\sqrt{2}a_{pc} \times \sqrt{2}a_{pc} \times 2c_{pc}$ structure, by an Fe atom along the c axis.

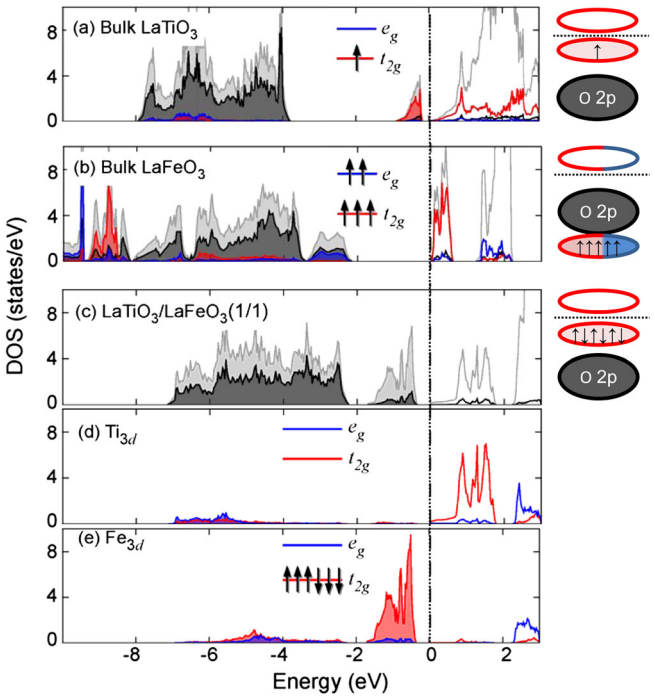

FIG. 1 (color online). Atomic and orbital projected DOS as well as schematic band structure of (a) bulk $LaTiO_3$, (b) bulk $LaFeO_3$, and (c)–(e) a (1/1) $LaTiO_3/LaFeO_3$ superlattice. Total states are marked in gray, O p states in black, Fe and Ti t_{2g} states in red, and Fe and Ti e_g states in blue. The Fermi level is indicated by the dotted line.

The atomic and orbital projected density of states (DOS) of a (1/1) $LaTiO_3/LaFeO_3$ superlattice are shown in Figs. 1(c)–1(e). At the interface, the nonbonding oxygen bands of $LaTiO_3$ and $LaFeO_3$ align [Fig. 1(c)], the Ti $3d$ bands are empty [Fig. 1(d)], and 6 electrons are located in the Fe $3d$ band [Fig. 1(e)]. This means that one electron is transferred from Ti to Fe, resulting in Ti^{4+} and Fe^{2+}. In addition, a rearrangement of the Fe $3d$ bands in the $LaTiO_3/LaFeO_3$ superlattice is observed. Here, a completely filled Fe t_{2g} band is located above the O $2p$ band and the Fe e_g band is empty [Fig. 1(e)], while in bulk the filled lower Hubbard band of Fe is below the O $2p$ band [Fig. 1(b)]. Because of the electron transfer and band rearrangement, a band insulator with a gap between the filled Fe t_{2g} and the empty Ti t_{2g} bands ($\Delta_B \approx 0.5$ eV) is formed at the interface [13]. In addition, the DFT results point to a magnetic transition: from $Ti^{3+}(t_{2g})$ and high-spin Fe^{3+} ($3t_{2g}\uparrow$, $2e_g\uparrow$) configuration in bulk to Ti^{4+} and low-spin Fe^{2+} ($3t_{2g}\uparrow$, $3t_{2g}\downarrow$) configuration (i.e., nonmagnetic) at the interface. To ensure that the observed charge transfer depended on the presence of partially filled d bands on both sides of the interface, we also calculated (1/1) and (2/2) $LaAlO_3/LaFeO_3$ superlattices. Here, no electron transfer or magnetic transition occurs, since Al has an empty $3d$ band well above the Fermi energy, which fixes the Al valence strictly to 3+ (see also Fig. 1 of Supplemental Material [23]).

According to the DFT results, the observed charge transfer at the $LaTiO_3/LaFeO_3$ interface is very robust. Increasing the thickness of $LaFeO_3$ to 4 u.c., slight straining of the unit cells, or varying $U_{\mathrm{Ti,Fe}}$ between 0 and 5 eV does not eliminate the observed transfer of one electron per interface unit cell. Moreover, investigating a (2/4) $LaTiO_3/LaFeO_3$ superlattice, it appears that the majority of transferred electrons remain at the $LaFeO_3$ interface layer [Figs. 2(c)–2(e) of Supplemental Material [23]). The layers farther away from the interface closely resemble the bulk DOS of $LaFeO_3$ [Fig. 1(b)]. Let us note that the interface charge transfer is very robust and reliable for any $LaFeO_3$ thickness. Even $LaTiO_3/LaFeO_3$ heterostructures without structural distortions show this one electron charge transfer (see Supplemental Material [23]). Since the charge transfer may lead to complex physical behavior in $LaFeO_3$, as a result of the competition of various magnetic configurations (bulk versus interface), it is difficult to accurately determine the magnetic and electronic state of interfaces where $LaFeO_3 > 2$ u.c.

The DFT results indicated that the interfacial electron transfer at $LaTiO_3/LaFeO_3$ interfaces is the consequence of (i) electrochemical potential, also described as O band alignment, and (ii) crystal field splitting and Hund's exchange. Taking only the O band alignment into account, electrons flow from Ti to Fe and reduce their electrochemical potential. As a result, an internal electric field, which balances the electrochemical potential difference between Ti and Fe, is created and prevents further charge transfer.

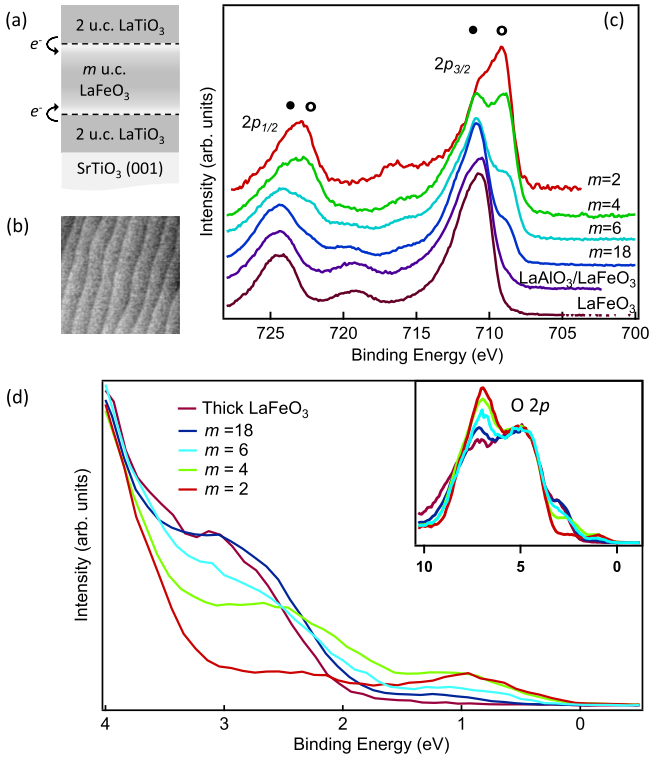

FIG. 2 (color online). (a) Sketch of the $LaTiO_3/LaFeO_3$ sample geometry. (b) A typical 1×1 μm AFM height image of a $LaTiO_3/LaFeO_3$ heterostructure. (c) Fe $2p$ XPS spectra of $LaTiO_3/LaFeO_3$ heterostructures for various thicknesses of $LaFeO_3$, as well as of a 30 u.c. $LaFeO_3$ film and a (2/2) $LaAlO_3/LaFeO_3$ heterostructure. The solid and open circles mark the Fe^{3+} and Fe^{2+} peaks, respectively. (d) Valence band XPS spectra of $LaTiO_3/LaFeO_3$ heterostructures for various thicknesses of $LaFeO_3$. All spectra were taken near normal emission ($\theta = 3°$).

This is also the reason why charge transfer at oxide interfaces is not evident when it only relies on O band alignment [24]. In $LaTiO_3/LaFeO_3$, however, an additional force comes into play, namely, a rearrangement of the Fe $3d$ bands. The origin of this rearrangement is a high-spin to low-spin transition, which is a result of the competition between Hund's exchange and crystal field splitting (see Supplemental Material [23]). This makes the low-spin configuration energetically more favorable for Fe^{2+} and yields an additional energy gain for the charge transfer. As a result, a strong electron transfer is observed at the $LaTiO_3/LaFeO_3$ interface and is accompanied by a loss of magnetic moment.

To resolve the predicted charge transfer and band rearrangement experimentally, we used XPS. XPS is very sensitive to variations in the valence state of transition metal ions and is able to detect the valence band structure. Therefore, it is a perfectly suited technique to determine the presence of both charge transfer and band rearrangement at the $LaTiO_3/LaFeO_3$ interface. We have studied $LaTiO_3/LaFeO_3$ heterostructures where the $LaFeO_3$ layer ($m = 2, 4, 6, 18$ u.c.) was sandwiched between two $LaTiO_3$ layers, each 2 u.c. thick [see Fig. 2(a)]. The heterostructures were grown on TiO_2-terminated $SrTiO_3$ (001) single crystals using pulsed laser deposition [25]. Commercial $LaFeO_3$ and $La_2Ti_2O_7$ sintered targets were ablated at a fluence of 1.9 J cm^{-2} and a repetition rate of 1 Hz. During growth, the substrate was held at 730 °C in 2×10^{-6} mbar oxygen atmosphere. Subsequently, the samples were cooled down to room temperature in 2×10^{-6} mbar oxygen. The low growth pressure was chosen to ensure the fabrication of the perovskite phase of $LaTiO_3$ [26].

The growth was *in situ* monitored by reflection high-energy electron diffraction (RHEED). Clear oscillations were observed during deposition and the RHEED pattern remained two dimensional [27]. Atomically smooth film surfaces with a defined terrace structure and one unit cell steps (~0.4 nm) were confirmed by atomic force microscopy (AFM) [see Fig. 2(b)]. X-ray diffraction reciprocal space maps showed that the heterostructures were fully strained and that the $LaTiO_3$ and $LaFeO_3$ u.c. volumes were similar to their bulk values. The volume conservation indicates that the heterostructures had a low defect density. The possible conducting behavior of the heterointerfaces could not be verified since the transport measurements were dominated by oxygen deficient $SrTiO_3$ as a result of the low pressure during growth and cooldown.

Directly after growth, the $LaTiO_3/LaFeO_3$ heterostructures were measured by *in situ* XPS [see Fig 2(c) and 2(d)]. The XPS system was equipped with an EA 125 electron energy analyzer. The measurements were done using a monochromized Al $K\alpha$ source (1486.6 eV). All spectra were aligned to the O $1s$ at 530.1 eV [29]. For analysis of the Fe $2p$ spectra, a Shirley background was subtracted and the spectra were normalized to the total area [30]. The valence band spectra were normalized to the intensity of the O $2p$ peak at 5 eV [31].

Figure 2(c) shows the Fe $2p$ spectra of $LaTiO_3/LaFeO_3$ heterostructures and a 30 u.c. thick $LaFeO_3$ film. The $LaFeO_3$ film exhibits a typical Fe^{3+} spectrum [32]. For the $LaTiO_3/LaFeO_3$ heterostructures, additional spectral weight is present at ~2 eV lower binding energy. This suggests that both Fe^{3+} and Fe^{2+} are present in the heterostructures and indicates that Fe reduction occurs adjacent to $LaTiO_3$. For comparison, only Fe^{3+} is observed in $LaFeO_3$ ($m = 2$) sandwiched between $LaAlO_3$ layers [Fig 2(c)]. Reducing the thickness of the $LaFeO_3$ layer in the heterostructures resulted in an increase of the Fe^{2+} signal, which confirms the DFT prediction that electron transfer occurs at $LaTiO_3/LaFeO_3$ interfaces. We also measured the Ti $2p$ spectra of the heterostructures to determine the presence of both Ti^{3+} to Ti^{4+}. Here, however, only a single peak for both the Ti $2p_{3/2}$ (at 459 eV) and Ti $2p_{1/2}$ spin-orbit peaks is observed. This could indicate a single Ti valence of presumably 4+ and hence complete charge transfer from Ti to Fe across the interface, independent of $LaFeO_3$

thickness in agreement with our DFT + U calculations (see Supplemental Material [23]) [33].

To quantify the total number of electrons transferred from $LaTiO_3$ to $LaFeO_3$ as well as the electron distribution across the $LaFeO_3$ layer, we performed angular resolved XPS measurements. By varying the emission angle θ with respect to the surface normal, we controlled the probing depth, i.e., controlled the effective electron escape depth $\lambda_{\text{eff}} = \lambda \cos\theta$, where λ is approximately 1.7 nm (see inset of Fig. 3) [34]. Next, we determined the Fe^{2+} and Fe^{3+} fractions of the Fe $2p$ spectra by decomposing the Shirley corrected spectra into an Fe^{2+} and Fe^{3+} component (see Supplemental Material for more details [23]). This resulted in a window of Fe^{2+} XPS signal for bulk ($\theta = 3°$) and surface ($\theta = 53°$) sensitive measurements, which is shown in Fig. 3. Both the decrease in spectral weight of Fe^{2+} for increasing $LaFeO_3$ thickness and the stronger Fe^{2+} signal in the surface sensitive measurements suggest that the transferred electrons are located near the $LaTiO_3/LaFeO_3$ interface. Note that the difference between the bulk and surface sensitive measurement for the $m = 2$ $LaTiO_3/LaFeO_3$ heterostructure would not be present if both $LaTiO_3/LaFeO_3$ interfaces behaved equally. For this specific sample, however, the deposition length of the top $LaTiO_3$ layer was 7% (2 pulses) longer than for the bottom $LaTiO_3$ layer. This may explain the difference between the bulk and surface sensitive measurements. In addition, the underlying $SrTiO_3/LaTiO_3$ interface may also reduce the total electron transfer from the bottom $LaTiO_3$ layer to the $LaFeO_3$ layer [4].

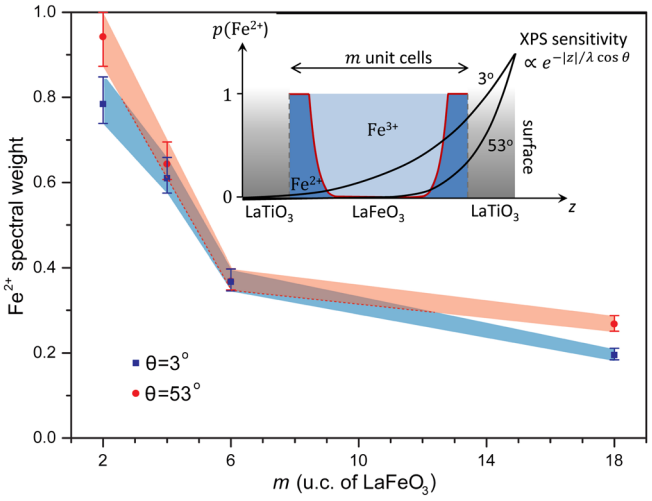

FIG. 3 (color online). Fe^{2+} spectral weight versus $LaFeO_3$ thickness for both bulk (blue) and surface (red) sensitive XPS measurements, taking $[Fe_{\text{total}}] = [Fe^{3+}] + [Fe^{2+}] = 1$. The inset is a schematic view of the Fe^{2+} fraction $[p(Fe^{2+})]$ across the $LaFeO_3$ layer (indicated by the solid red curve). Fe^{2+} (Fe^{3+}) fraction is given in dark (light) blue. In addition, an indication of the XPS sensitivity for both surface (53°) and bulk (3°) sensitive measurements is shown. z indicates the direction perpendicular to the surface.

Subsequently, we determined the total electron transfer and electron distribution by modeling the thickness dependence of the spectral weight of Fe^{2+} shown in Fig. 3. This was done by iteratively optimizing the electron doping in the five $LaFeO_3$ layers nearest to the interface with $LaTiO_3$ between 0 and 1 (for more details see Supplemental Material [23]). This model confirmed that the majority of transferred electrons was located in the $LaFeO_3$ layer closest to the interface as well as that the number of electrons rapidly decreased for layers farther away from the interface (see inset of Fig. 3). These findings are in good agreement with our DFT results, where for thicker $LaFeO_3$ layers also a minor part of the electrons is transferred to the $LaFeO_3$ layers away from the interface [see Fig. 2(e) of the Supplemental Material [23]]. In addition, the model gave an indication of the total electron transfer, from 0.8–1.0 e^-/interface u.c. for $m = 2$ heterostructures to 1.1–1.4 e^-/interface u.c. for heterostructures with $m > 10$. The total electron transfer $> 1e^-$/interface u.c. indicates that additional electrons are transferred from the $LaTiO_3$ layers farther away from the interface. This is also suggested by our DFT results taking Ti surface states into account (see Supplemental Material [23]). In comparison to our DFT results, the total charge transfer observed experimentally is significantly higher. However, for the DFT calculations a (1/1) system was used, thus all $LaTiO_3$ layers were adjacent to $LaFeO_3$, and therefore, the number of transferred electrons could not exceed 1 e^-/interface u.c. Let us note that possible Ti/Fe intermixing across the interface may affect the exact electron distribution and total charge transfer, but does not change the essential interface physics (see also Supplemental Material [23]).

Next to electron transfer, our DFT calculations predict rearrangement of the Fe $3d$ bands. To study this rearrangement, we measured the valence band spectra by XPS [Fig. 2(d)] [31]. Comparing the spectra of $LaTiO_3/LaFeO_3$ heterostructures with the spectra of the thick $LaFeO_3$ film, a new peak at 1 eV is present for the heterostructures. According to the DFT calculations, this new peak is attributed to the completely filled t_{2g} band of Fe^{2+}. The intensity of this peak depends on the number of strongly electron doped $LaFeO_3$ layers near the surface. Taking the electron distribution in $LaFeO_3$ into account, the first two $LaFeO_3$ layers nearest to the $LaTiO_3/LaFeO_3$ interface would mainly contribute to the spectral weight of this peak. This also explains the similar peak intensity for the $m = 2$ and $m = 4$ heterostructures but reduced intensity for the thicker heterostructures. Simultaneously, the charge transfer band of $LaFeO_3$, resulting from the O $2p$-Fe e_g hybridization, decreases in intensity. This strongly supports the occurrence of Fe band rearrangement at the $LaTiO_3/LaFeO_3$ interface predicted by DFT. The presence of Fe band rearrangement strongly indicates that the interfaces become nonmagnetic, as proposed by our DFT calculations.

In addition, the Ti $3d^1$ band near the Fermi level may be present in the valence band spectra. However, the resulting changes in the Ti $3d$ occupation of the $LaTiO_3$ layers are difficult to extract from the spectra shown in Fig. 2(d), as the Ti $3d^1$ peak is very weak and probably obscured by the appearance of the new Fe peak [35].

In conclusion, we have shown that the competition between electrochemical potential, crystal field splitting, and correlation energy can lead to an unprecedented transfer of electrons at $LaTiO_3/LaFeO_3$ interfaces. Using XPS, we showed a charge transfer up to $1.2 \pm 0.2e^-$/interface u.c. from Ti to Fe as well as the rearrangement of the Fe $3d$ bands. For $LaTiO_3/LaFeO_3$, the charge transfer suppresses the magnetic moment and antiferromagnetism at the interface. Considering the basic electronic configuration, we expect, however, the interfaces of, e.g., $LaTiO_3/LaMnO_3$ and $LaTiO_3/LaCoO_3$ to become ferromagnetic upon charge transfer. Moreover, by applying biaxial strain, it may be possible to control the number of transferred electrons and, with it, the interfacial properties. Hence, the reported charge transfer up to 1.2 ± 0.2 e^-/interface u.c. opens novel routes to design functional oxide interfaces.

The authors thank B. Kuiper for valuable technical help. G. R. thanks The Netherlands Organization for Scientific Research (NWO) for financial support through a VIDI grant. R. C. and K. H. acknowledge support from Research Unit FOR 1346 of the Deutsche Forschungsgemeinschaft and the Austrian Science Fund (project ID I597), respectively.

*Present address: Department of Materials Science and Metallurgy, University of Cambridge, Cambridge CB3 0FS, United Kingdom.
jek46@cam.ac.uk

[1] K. Ueda, H. Tabata, and T. Kawai, Phys. Rev. B **60**, R12561 (1999).
[2] A. Gozar, G. Logvenov, L. Fitting Kourkoutis, A. T. Bollinger, L. A. Giannuzzi, D. A. Muller, and I. Bozovic, Nature (London) **455**, 782 (2008).
[3] A. Ohtomo and H. Y. Hwang, Nature (London) **427**, 423 (2004).
[4] A. Ohtomo, D. A. Muller, J. L. Grazul, and H. Y. Hwang, Nature (London) **419**, 378 (2002).
[5] P. Moetakef, T. A. Cain, D. G. Ouellette, J. Y. Zhang, D. O. Klenov, A. Janotti, C. G. Van de Walle, S. Rajan, S. J. Allen, and S. Stemmer, Appl. Phys. Lett. **99**, 232116 (2011).
[6] S. Okamoto and A. Millis, Nature (London) **428**, 630 (2004).
[7] N. Nakagawa, H. Y. Hwang, and D. A. Muller, Nat. Mater. **5**, 204 (2006).
[8] C. Noguera, J. Phys. Condens. Matter **12**, R367 (2000).
[9] A. Kalabukhov, R. Gunnarsson, J. Börjesson, E. Olsson, T. Claeson, and D. Winkler, Phys. Rev. B **75**, 121404 (2007).
[10] W. Siemons, G. Koster, H. Yamamoto, W. A. Harrison, G. Lucovsky, T. H. Geballe, D. H. A. Blank, and M. R. Beasley, Phys. Rev. Lett. **98**, 196802 (2007).
[11] Z. Zhong, P. X. Xu, and P. J. Kelly, Phys. Rev. B **82**, 165127 (2010).
[12] Y. Chen, N. Pryds, J. E. Kleibeuker, G. Koster, J. Sun, E. Stamate, B. Shen, G. Rijnders, and S. Linderoth, Nano Lett. **11**, 3774 (2011).
[13] J. Zaanen, G. A. Sawatzky, and J. W. Allen, Phys. Rev. Lett. **55**, 418 (1985).
[14] T. Arima, Y. Tokura, and J. B. Torrance, Phys. Rev. B **48**, 17 006 (1993).
[15] H. Chen, A. J. Millis, and C. A. Marianetti, Phys. Rev. Lett. **111**, 116403 (2013).
[16] P. E. Blochl, Phys. Rev. B **50**, 17 953 (1994).
[17] G. Kresse and D. Joubert, Phys. Rev. B **59**, 1758 (1999).
[18] S. L. Dudarev, G. A. Botton, S. Y. Savrasov, C. J. Humphreys, and A. P. Sutton, Phys. Rev. B **57**, 1505 (1998).
[19] Y. Tokura, Y. Taguchi, Y. Okada, Y. Fujishima, T. Arima, K. Kumagai, and Y. Iye, Phys. Rev. Lett. **70**, 2126 (1993).
[20] W. C. Koehler, E. O. Wollan, and M. K. Wilkinson, Phys. Rev. **118**, 58 (1960).
[21] E. Pavarini, S. Biermann, A. Poteryaev, A. I. Lichtenstein, A. Georges, and O. K. Andersen, Phys. Rev. Lett. **92**, 176403 (2004).
[22] Z. Zhong and P. J. Kelly, Europhys. Lett. **84**, 27 001 (2008).
[23] See Supplemental Material at http://link.aps.org/supplemental/10.1103/PhysRevLett.113.237402 for additional data and analysis of results in this Letter.
[24] P. Zubko, S. Gariglio, M. Gabay, P. Ghosez, and J.-M. Triscone, Annu. Rev. Condens. Matter Phys. **2**, 141 (2011).
[25] G. Koster, B. L. Kropman, G. J. H. M. Rijnders, D. H. A. Blank, and H. Rogalla, Appl. Phys. Lett. **73**, 2920 (1998).
[26] A. Ohtomo, D. A. Muller, J. L. Grazul, and H. Y. Hwang, Appl. Phys. Lett. **80**, 3922 (2002).
[27] Note that some Ti/Fe intermixing across the interface may be present, taking the low oxygen pressure during growth into account [28].
[28] P. R. Willmott, S. A. Pauli, R. Herger, C. M. Schlepütz, D. Martoccia, B. D. Patterson, B. Delley, R. Clarke, D. Kumah, C. Cionca, and Y. Yacoby, Phys. Rev. Lett. **99**, 155502 (2007).
[29] No charging of the samples was observed during x-ray exposure since the $SrTiO_{3-\delta}$ became conducting as a result of the low oxygen pressure during growth and cooldown.
[30] The La MNN Auger peak (at ~740 − 800 eV) obscures the Fe $2p$ satellite structure at higher binding energy. To allow proper normalization, we limited the Fe $2p$ range up to this satellite peak.
[31] Normalization of the valence band spectra is complicated by the Ti-O $2p$ and Fe-O $2p$ hybridization. To allow for a qualitative analysis, the valence band spectra were aligned on the intensity of the O $2p$ at 5 eV. However, this may result in minor normalization artifacts.
[32] T. Fujii, F. M. F. de Groot, G. A. Sawatzky, F. C. Voogt, T. Hibma, and K. Okada, Phys. Rev. B **59**, 3195 (1999).
[33] M. Kareev, Y. Cao, X. Liu, S. Middey, D. Meyers, and J. Chakhalian, Appl. Phys. Lett. **103**, 231605 (2013).
[34] NIST Standard Reference Database 71, version 2.1.
[35] M. Takizawa, H. Wadati, K. Tanaka, M. Hashimoto, T. Yoshida, A. Fujimori, A. Chikamatsu, H. Kumigashira, M. Oshima, K. Shibuya, T. Mihara, T. Ohnishi, M. Lippmaa, M. Kawasaki, H. Koinuma, S. Okamoto, and A. J. Millis, Phys. Rev. Lett. **97**, 057601 (2006).